PLOS ONE

Mixed convective flow of a magnetohydrodynamic Casson fluid through a permeable stretching sheet with first-order chemical reaction

Anwar Saeed[1], Ebrahem A. Algehyne[2,3], Musaad S. Aldhabani[2], Abdullah Dawar[4], Poom Kumam[1,5]*, Wiyada Kumam[6]

1 Center of Excellence in Theoretical and Computational Science (TaCS-CoE), Faculty of Science, King Mongkut's University of Technology Thonburi (KMUTT), Bang Mod, Thung Khru, Bangkok, Thailand, 2 Department of Mathematics, Faculty of Science, University of Tabuk, Tabuk, Saudi Arabia, 3 Nanotechnology Research Unit (NRU), University of Tabuk, Tabuk, Saudi Arabia, 4 Department of Mathematics, Abdul Wali Khan University, Mardan, Khyber Pakhtunkhwa, Pakistan, 5 Department of Medical Research, China Medical University Hospital, China Medical University, Taichung, Taiwan, 6 Applied Mathematics for Science and Engineering Research Unit (AMSERU), Program in Applied Statistics, Department of Mathematics and Computer Science, Faculty of Science and Technology, Rajamangala University of Technology Thanyaburi, Thanyaburi, Pathumthani, Thailand

* poom.kum@kmutt.ac.th

Abstract

This research article presents the magnetohydrodynamic Casson fluid flow through an extending surface embedded in a porous medium. Furthermore, the Casson fluid flow is investigated under the effects of thermal radiation, Joule heating, viscous dissipation, and chemical reaction. The analytical solution of the modeled problem is utilized with the help of homotopy analysis method (HAM). The convergence region of the applied technique is portrayed graphically. The impacts of the embedded factors on the flow profiles are exhibited with the help of figures. Furthermore, numerical values of the surface drag force, heat, and mass transfer rates are highlighted via table. The results show that the augmented Darcy number, Casson and magnetic parameters have declined the velocity profile of the Casson fluid flow. Growth in Brownian motion augments the chaotic motion amongst the particles due to which the kinetic energy of the particles transforms to heat energy which consequently augmented the thermal profile, while reduced the concentration profile. The mass and energy profiles are positively effects with the increment of thermophoresis term. And the growing values of chemical reaction and Lewis number cause a reduction in the diffusivity of mass of fluid due to which less transfer of mass takes place that weakens the concentration layer thickness and declines the concentration profiles.

1. Introduction

During the past few decades, the mass and heat transmission past a permeable and extending sheet has achieved a significant response from numerous researchers for its important

applications in industry and engineering technology. Carbonell and Whitaker [1] inspected the transmission of heat and mass for permeable medium with the main focus on the energy and concentration equations in their study. Yaglom and Kader [2] have investigated the transportation of mass and heat within a turbulent fluid flow and a rough wall by employing a high Reynolds number. It has been observed in this work that, more disturbances have been produced due to the roughness of the wall that has augmented the transmission of heat and mass in comparison to a smooth wall at similar values of Prandtl and Reynolds numbers. Bandaru et al. [3] have scrutinized the thermal and mass flow from a rotary cone to fluid transport through a permeable medium by using thermophoresis and nonlinear convective impacts. The thermal flow is more prominent and influential than mass transportation. Krishna et al. [4] have used a permeable vertical sheet to investigate the temperature and concentration for a second grade fluid. Ahmad et al. [5] observed the transportation of heat for hybrid nanoparticles flow upon a porous surface.

In fluid flows, the transportation characteristics have been described by two different models that are Buongiorno model [6] and Das, Tiwari model [7]. The main focus in the former model is upon the upsots of thermophoresis and Brownian motion regarding the flow of fluid under the influence of numerous flow conditions. Khan et al. [8–11] conducted remarkable work in the field of energy and mass transference for fluid flow employing different geometrical and several flow conditions views. It has been highlighted in these investigations that the energy field has augmented by varying the Brownian motion parameter and thermophoretic effects, which on the other hand has declined the mass flow rate. Mittal and Petal [12] have discussed the impacts of these two terms over mixed convection bi-dimensional MHD fluid flow by taking the heat generation and nonlinear radiations. It has been observed in this study that the concentration characteristics have declined while the thermal profile upsurge with augmented values of thermophoretic. Ashraf et al. [13] have inspected the effects of these two terms upon the flow of fluid using viscous dissipation in the closed vicinity of the stagnation point. Abdelmalek et al. [14] have used the electrically conducted visco-inelastic nanoparticles flow on a stretching surface under the influences of thermophoretic effects. It has been detected in this inspection that flow has reduced and thermal profiles have increased with augmentation in magnetic strength. Rashidi et al. [15] presented the comprehensive analysis of the thermophysical properties of hybrid nanofluids. Mahdi and Nazari [16] investigated the water-based Ag nanofluid flow by using an artificial neural network.

The combination of chemical reactions with the analysis of energy and mass allocation plays a momentous role in flow problems. For its importance and extensive applications, it attained the remarkable attention of researchers and scientists in the last few decades. These applications include different engineering progressions such as cooling of electrical equipment and devices, transpiration of humans, chemically catalytic reactors and aircraft propulsion devices, etc. Gangadhar and Bhaskar [17] have presented a two-dimensional mathematical model to discuss the thermal and mass flow for MHD fluid flow upon a porous and expanded surface. It has been revealed in this work that, the flow profile has declined sharply due to growth in the magnetic field while the thermal flow has amplified in this process. Seth et al. [18] inspected the upshot of chemical reactions upon thermal and mass transmission for convective fluid flow past a moving porous sheet. In this work, a closed form solution has been obtained for flow, energy, and concentration equations by using Laplace transformation. Moreover, the descriptions for Sherwood and Nusselt numbers have also been determined in this work. Reddy et al. [19] have presented the profiles of thermal and mass transmission for MHD fluid flow by using chemical reactions on a rotating permeable disk. The thermal radiation upshot and partial slip has also been incorporated in this work and has established that flow has reduced while thermal flow has improved with the increment of solid nanoparticles.

Raju [20] has inspected the time dependent MHD fluid flow on a penetrable and inclined sheet by considering the chemical reaction upshots in the concentration equation. In this study, the Darcian flow model for permeable surfaces has also been used in the flow system. Punith Gowda et al. [21] surveyed the fluid flow and heat communication for non-Newtonian fluid using a chemical reaction. The results of this work revealed that flow has augmented and thermal profile has declined with escalating values of Marangoni number. Moreover, it has been perceived that the flow profiles condensed with the expansion in permeability term. The readers can further study the effects and benefits of chemical reactions upon fluid flow system in Refs [22–26].

A surface that contains small void spaces (pores) is characterized as a permeable surface. The idea of the porous medium is extensively used in applied sciences such as filtration purposes, petroleum engineering, petroleum geology, geophysics, biophysics, and biology, etc. Due to its importance in the field of applied sciences, many investigations have been carried out with the core focal point on thermal flow and transference of mass in fluid motion upon the porous medium. Bejan and Khair [27] have discussed the heat transition for the fluid flow over a porous texture. Chaudhary and Jain [28] have investigated the fluid flow past a plate implanted in a permeable region. It has been established in this investigation that magnetic effects have supported the thermal characteristics and have opposed the flow of fluid. Jiang et al. [29] reviewed the MHD unsteady flow of fluid inside a penetrable surface with the influence of Hall current upon thermal flow. The concept of fractional derivative along with constitutive equations has been employed in this work. Kumar et al. [30] have inspected the cross flow for MHD fluid upon an accelerating upright surface in an absorbent surface using Hall current. It has been observed in this work that mass transfer of fluid has been maintained by enlarging credit of Soret number and has been opposed with augmentation in Dufour number. A comparative study has also been carried out in this investigation with a fine agreement with published results. Haq et al. [31] scrutinized the convective thermal flow of ferrofluid across a porous exterior. In this study, the thermal radiation has been incorporated in the temperature equation that has supported the flow and temperature profile.

After a careful review of the above literature, we are in a position to present the steady and incompressible two-dimensional flow of magnetohydrodynamic Casson fluid through an extending sheet inserted in an absorbent medium. The fluid flow has exposed with the impacts of Brownian motion and thermophoresis by using the idea of Buongiorno's model. The influence of chemical reaction has also been incorporated mathematically in the concentration equation. At the end of this analysis, we will respond to the subsequent research queries.

1. Does the Casson parameter strengthen the momentum boundary layer?

2. How does the Casson fluid flow behave against the magnetic field using porous media?

3. How does the Casson fluid flow behave against the thermophoretic and Brownian motion parameters?

4. What is the effect of Darcy number on the thermal profile of the Casson fluid flow?

5. What is the impact of chemical reaction constraint on the mass profile of the Casson fluid flow?

2. Problem formulation

Consider the steady and incompressible magnetohydrodynamic and thermally radiative flow of Casson fluid across a stretching sheet embedded in a permeable medium. The extending
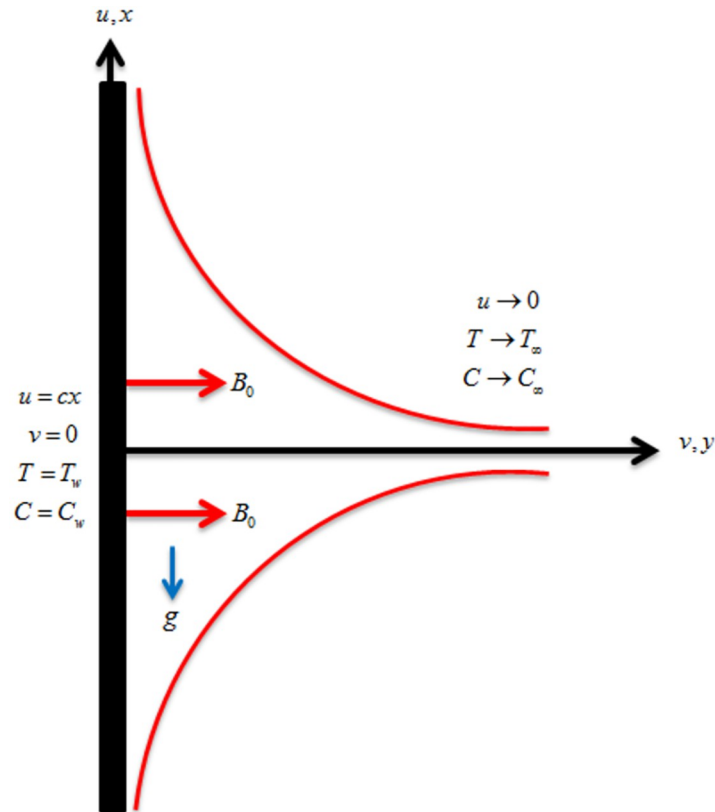
Fig 1. Geometry of the fluid flow.

https://doi.org/10.1371/journal.pone.0265238.g001

velocity of the sheet is defined as $u_w = ax$ where a is the positive constant. In the xy–plane, x is taken along the sheet and y is taken perpendicular to the stretching sheet as shown in Fig 1. A magnetic field of strength B_0 is applied normal to the fluid flow. The gravitational force g acts in downward direction. The surface temperature is represented by T_w whereas the ambient temperature is signified by T_∞. Also, the surface and ambient concentrations are respectively represented by C_w and C_∞. The leading equations are defined as [32, 33]:

$$\frac{\partial u}{\partial x} + \frac{\partial v}{\partial y} = 0, \tag{1}$$

$$u\frac{\partial u}{\partial x} + v\frac{\partial u}{\partial y} = \frac{\mu_f}{\rho_f}\left(1+\frac{1}{\beta}\right)\frac{\partial^2 u}{\partial y^2} - \frac{\sigma B_0^2}{\rho_f}u - \frac{\mu_f}{\rho_f K}u + \frac{g}{\rho_f}\left[\rho_f\beta(T-T_\infty) - \left(\rho_p - \rho_f\right)(C-C_\infty)\right], \tag{2}$$

$$u\frac{\partial T}{\partial x} + v\frac{\partial T}{\partial y} = \alpha_f\left(1+\frac{16\sigma^* T_\infty^3}{3kk^*}\right)\frac{\partial^2 T}{\partial y^2} + \tau D_B\left(\frac{\partial T}{\partial y}\frac{\partial C}{\partial y}\right) + \frac{\tau D_T}{T_\infty}\left(\frac{\partial T}{\partial y}\right)^2 + \frac{\alpha_f\mu_f}{k}\left(\frac{\partial u}{\partial y}\right)^2 + \left(\frac{\alpha_f\sigma B_0^2}{k} + \frac{\alpha_f\mu_f}{kK}\right)u^2, \tag{3}$$

$$u\frac{\partial C}{\partial x} + v\frac{\partial C}{\partial y} + kr(C-C_\infty) = D_B\frac{\partial^2 C}{\partial y^2} + \frac{D_T}{T_\infty}\frac{\partial^2 T}{\partial y^2}, \tag{4}$$

with boundary conditions:

$$
\left.\begin{array}{l}
u = ax, \quad v = 0, \quad T = T_w, \quad C = C_w \quad at \quad y = 0 \\
u \rightarrow 0, \quad T \rightarrow T_\infty, \quad C \rightarrow C_\infty \quad as \quad y \rightarrow \infty
\end{array}\right\}, \tag{5}
$$

Here, the velocity components are u and v along x– and y–directions respectively, ν_f is the kinematic viscosity, ρ_p is the density of the nanoparticle, ρ_f is the density of the fluid, D_B is coefficient of Brownian diffusion, D_T is the coefficient of thermophoresis diffusion, α_f is the thermal diffusivity, kr is the chemical reaction term, C is the concentration, T is the temperature, C_w is the surface concentration and μ_f is the fluid viscosity.

The correspondence transformations are defined as [34]:

$$
\psi(x, y) = \alpha_f Ra_x^{1/4} f(\xi), \quad u = \frac{\partial \psi}{\partial y}, \quad v = -\frac{\partial \psi}{\partial x}, \quad \theta(\xi) = \frac{T - T_\infty}{T_w - T_\infty}, \quad \phi(\xi) = \frac{C - C_\infty}{C_w - C_\infty}, \quad \xi = \frac{y}{x} Ra_x^{1/4}. \tag{6}
$$

Using the above resemblance substitution, the leading equations are reduced as:

$$
\left(1 + \frac{1}{\beta}\right) f''' + \frac{1}{4\mathrm{Pr}} \left(-2f'^2 + 3ff''\right) - \left(M + \frac{1}{Da}\right) f' - Nr\phi + \theta = 0, \tag{7}
$$

$$
\left(1 + \frac{4}{3} Rd\right) \theta'' + \frac{3}{4} f\theta' + Ec\, \mathrm{Pr} \left(f''^2 + \left(M + \frac{1}{Da}\right) f'^2\right) + Nb\theta'\phi' + Nt\theta'^2 = 0, \tag{8}
$$

$$
\phi'' + \frac{Nt}{Nb} \theta'' + \frac{3}{4} Lef\phi' - LeK\phi = 0, \tag{9}
$$

with

$$
f(0) = 0, \ f'(0) = \lambda, \ \phi(0) = 1, \ \theta(0) = 1, \ f'(\infty) = 0, \ \phi(\infty) = 0, \ \theta(\infty) = 0. \tag{10}
$$

Here, the magnetic parameter is indicated by $M\left(= \frac{\sigma_f B_0^2 x^2}{\mu_f Ra_x^{1/2}}\right)$, Eckert number is denoted by $Ec\left(= \frac{u_w^2}{C_{pf}(T_w - T_\infty)}\right)$, thermal radiation is represented by $Rd\left(= \frac{4\sigma^* T_\infty^3}{kk^*}\right)$, Prandtl number is signified by $\mathrm{Pr}\left(= \frac{\nu_f}{\alpha_f}\right)$, Brownian motion is indicated by $Nb\left(= \frac{\tau D_B(C_w - C_\infty)}{\alpha_f}\right)$, $Nr\left(= \frac{(\rho_p - \rho_f)(C_w - C_\infty)}{\rho_f \beta(T_w - T_\infty)}\right)$ is the buoyancy ratio parameter, thermophoresis term is denoted by $Nt\left(= \frac{\tau D_T(T_w - T_\infty)}{\alpha_f T_\infty}\right)$, the stretching/shrinking parameter is indicated by $\lambda\left(= \frac{ax^2}{Ra_x^{1/2}\alpha_f}\right)$, Lewis number is denoted by $Le\left(= \frac{\alpha_f}{D_B}\right)$, and the porous medium parameter is represented by $Da\left(= \frac{KRa_x^{1/2}}{x^2}\right)$.

The mathematical expressions for the physical quantities are stated as:

$$
C_f = \frac{\tau_w}{\mu_f \alpha_f Ra_x^{3/4}}, \quad Nu = \frac{1}{k} \frac{xq_w}{(T_w - T_\infty)}, \quad Sh = \frac{1}{D_B} \frac{xq_m}{(C_w - C_\infty)}, \tag{11}
$$

where τ_w, q_w and q_m are rebound as:

$$
\tau_w = \left(1 + \frac{1}{\beta}\right) \frac{\partial u}{\partial y}\bigg|_{y=0}, \quad q_w = -\left(k + \frac{16\sigma^* T_\infty^3}{3k^*}\right) \frac{\partial T}{\partial y}\bigg|_{y=0}, \quad q_m = -D_B \frac{\partial C}{\partial y}\bigg|_{y=0}. \tag{12}
$$

Eq (11) is reduced as:

$$C_f Ra_x^{1/4} = \left(1 + \frac{1}{\beta}\right) f''(0), \quad \frac{Nu}{Ra_x^{1/4}} = -\left(1 + \frac{4}{3} Rd\right) \theta'(0), \quad \frac{Sh}{Ra_x^{1/4}} = -\phi'(0),$$ (13)

where $Ra_x = \frac{(1-\varphi)g\beta(T_w - T_\infty)x^3}{v_f \alpha_f}$ is the local Rayleigh number.

3. HAM solution

The initial guesses and linear operators are taken as:

$$f_0(\xi) = \lambda\left(1 - e^{-\xi}\right), \quad \theta_0(\xi) = e^{-\xi}, \quad \phi_0(\xi) = e^{-\xi}.$$ (14)

$$L_f = f''' - f', \quad L_\theta = \theta'' - \theta, \quad L_\phi = \phi'' - \phi.$$ (15)

with properties:

$$L_f\left(q_1 + q_2 e^{\xi} + q_3 e^{-\xi}\right) = 0, \quad L_\theta\left(q_4 e^{\xi} + q_5 e^{-\xi}\right), \quad L_\phi\left(q_6 e^{\xi} + q_7 e^{-\xi}\right) = 0,$$ (16)

where $q_1 - q_7$ are the constants of general solution.

4. HAM convergence

HAM provides the convergence of the series solutions. The auxiliary factor $\hbar$ performs an important character in adjusting and controlling the region of convergence of our series solutions. Thus, we have schemed the $\hbar$–curves for $f'(\xi)$, $\theta(\xi)$ and $\phi(\xi)$ in Fig 2. The region of convergence for $f'(\xi)$, $\theta(\xi)$ and $\phi(\xi)$ are $0.25 \leq \hbar_f \leq 0.0$, $-0.32 \leq \hbar_\theta \leq 0.05$ and $-0.34 \leq \hbar_\phi \leq 0.1$ respectively.

5. Discussion of results

This work describes the improvement of energy and mass transmission for a mixed convection Casson fluid flow upon an extending sheet using an absorbent medium. The fluid flow has exposed the impressions of thermophoresis and Brownian motion by using the idea of Buongiorno's model. The influence of chemical reaction has also been incorporated mathematically in the concentration equation. The equations that regulated the flow problem have
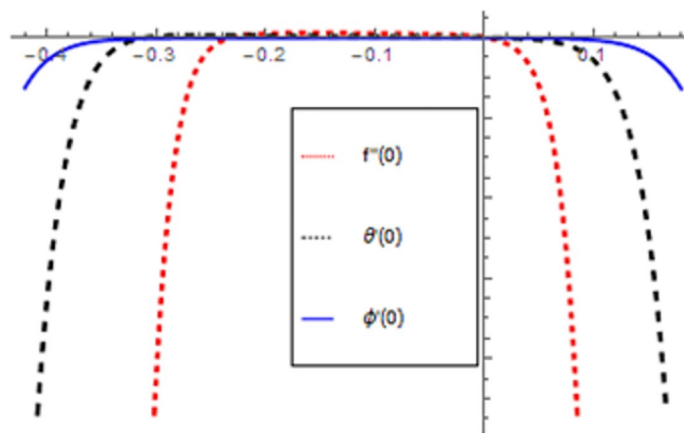

**Fig 2.** $\hbar$–curves for $f'(\xi)$, $\theta(\xi)$ and $\phi(\xi)$.

Table 1. Validation of the skin friction values with previously published results when $M = 1.0$, $Ec = 0.1$, $Da \to \infty$, and $\beta \to \infty$.

| Nr	λ	$f''(0)$	
		Makinde et al. [34]	Presents results
0.0	-0.5	2.35476	2.354765
0.3		2.21267	2.212673
0.5		2.11589	2.115891
0.0	0.0	1.73117	1.731173
0.3		1.60462	1.604624
0.5		1.51848	1.518482
0.0	0.5	1.03430	1.034305
0.3		0.92053	0.920532
0.5		0.84380	0.843801

transformed to dimensionless notation with suitable similarity variables. The solution has been determined by HAM. The codes for HAM are incorporated in MATHEMATICA 12.0 software. The authentication of the present analysis is represented by Table 1. The effect of various substantial constraints on the fluid flow profiles has been reviewed in the subsequent lines. To support our discussion, a graphical view of different profiles has also been presented.

Fig 3 portrays the influence of Darcy number Da and Casson parameter β upon the velocity profiles. It has been spotted from this figure that with enlargement in Darcy number the void spaces in the surface will increase that offers more resistance to the fluid motion. In this physical phenomenon, the velocity characteristics decline. On the other hand, the declining impact of Casson coefficient β on the velocity field is depicted. The reason behind the declining impact on velocity profile is that the augmenting Casson parameter augments the viscosity of the fluid flow which yields the reduction in velocity of the fluid flow. Also, the increasing Casson
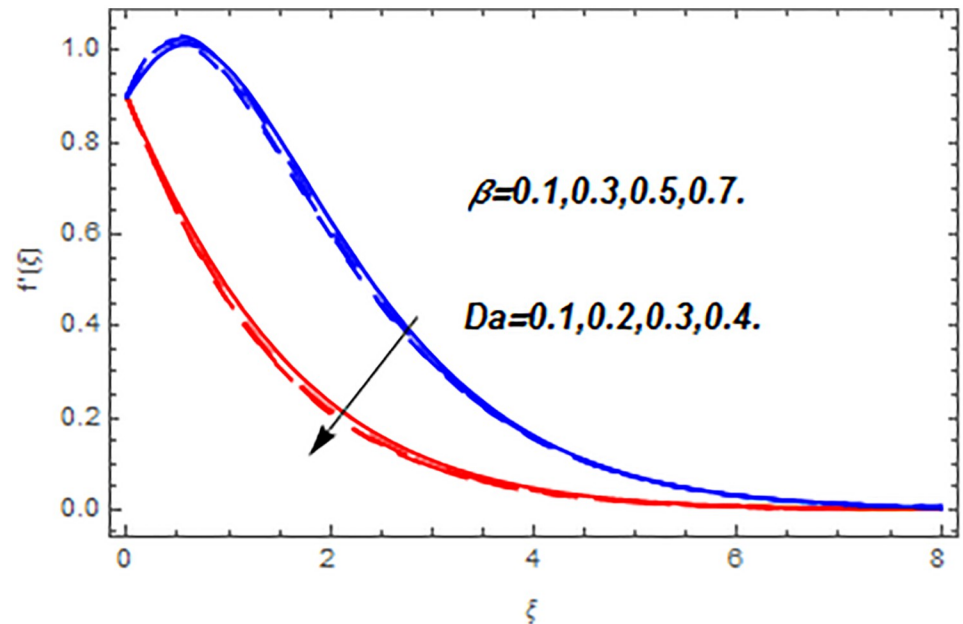
**Fig 3. Flow profiles versus Darcy number and Casson parameter.**
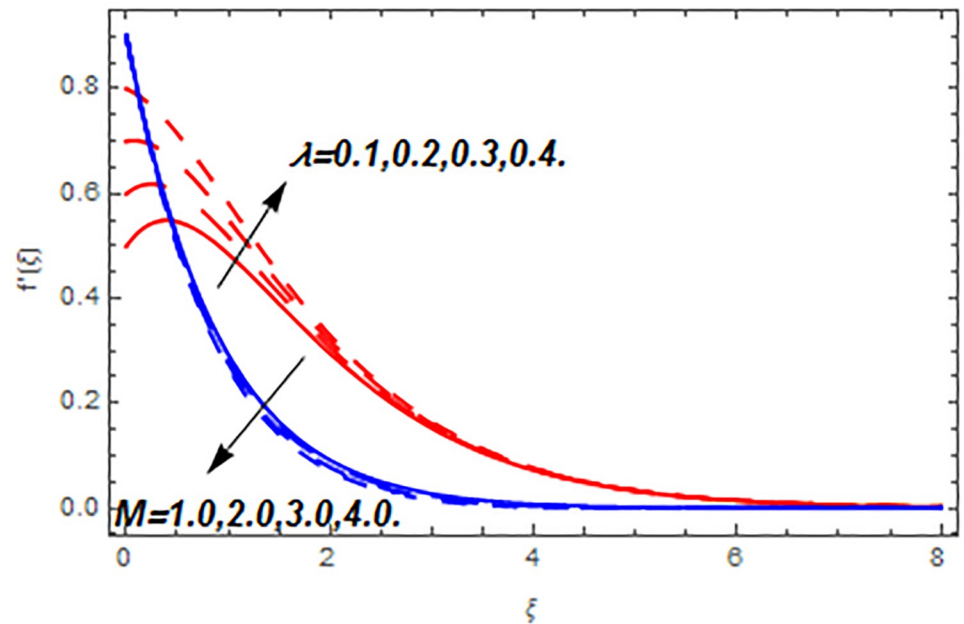
**Fig 4. Flow profiles versus magnetic and stretching parameters.**

https://doi.org/10.1371/journal.pone.0265238.g004

parameter (say $\beta \to \infty$) leads to the viscous fluid. Fig 4 reveals the influence of magnetic M and stretching constraint λ upon the velocity field. Since an augmentation in the values of M creates the Lorentz force which produces the opposing force to the fluid flow. This opposing force reduces the velocity of the fluid flow. Therefore, a declining effect of magnetic term is depicted. On the other hand the growth in λ leads to an augmentation in the flow of fluid. It is obvious that the increasing stretching parameter augments the stretching phenomenon of the proposed geometry which consequently augments the velocity of the fluid. Thus an augmenting impact is observed here. Fig 5 presents the upshot of Brownian motion and thermophoresis upon energy profile. An augmentation in Nb grows up the thermal flow of fluid. Actually,
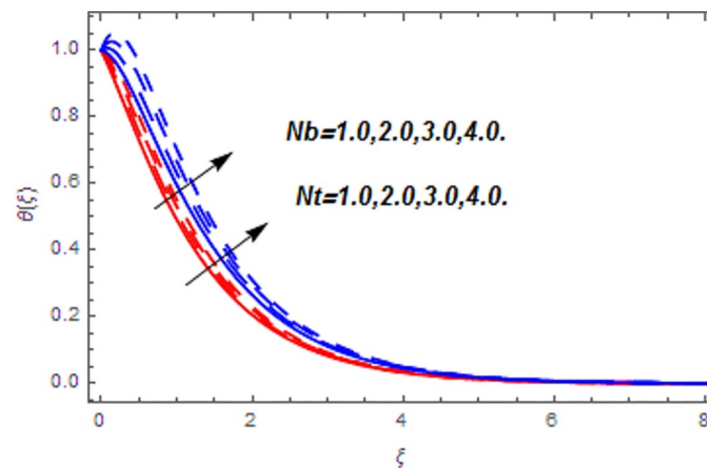
Fig 5. Thermal profiles versus Brownian motion and thermophoresis parameters.

https://doi.org/10.1371/journal.pone.0265238.g005
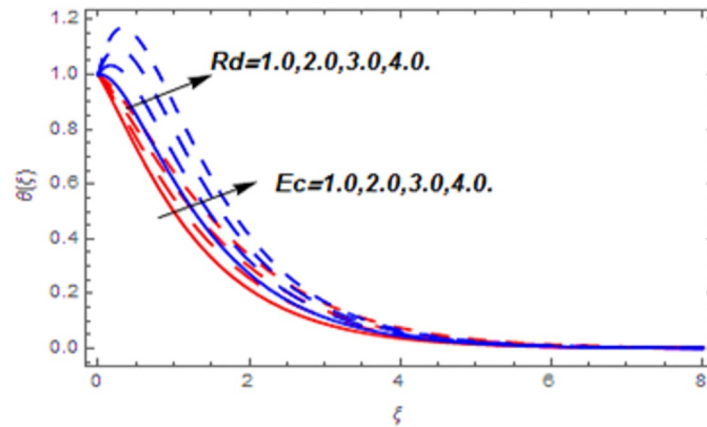
**Fig 6. Thermal profiles versus Eckert number and radiation parameter.**

it can be explained as a growth in Nb augments the chaotic motion amongst the particles, due to which the kinetic energy of the particles transform to heat energy. In this process the thermal profile of the particles grow up. Similarly, a growth in thermophoresis constant Nt supports the energy field. Actually for upsurge values of Nt the difference in temperature of the fluid grows up due to which more heat will transfer from hotter to colder region. Hence augmentation in Nt increases the thermal profile for fluid flow system. Fig 6 depicts the behavior of thermal profile in response of Eckert number Ec and radiation Rd. For augmenting values of Ec the transport energy of fluid flow system grows up that causes the alteration of kinetic energy to heat energy. In this physical phenomenon the thermal profiles upsurge. Similarly growth in radiation parameter pushes the temperature of the fluid in forward direction. Actually, growth in Rd causes a maximum release of heat energy to flow direction that gives strength to the thickness of thermal layer, and ultimately grows up the thermal flow profile. Fig 7 portrays the influence of Darcy number Da and magnetic parameter M upon thermal profiles. The higher values of Da causes a higher permeability in porous surface that leads to a drop down in thermal conduction. In this physical phenomenon the thermal profiles decline. Fig 7 also depicts an upsurge in thermal profile due to growth in magnetic field. Actually, the
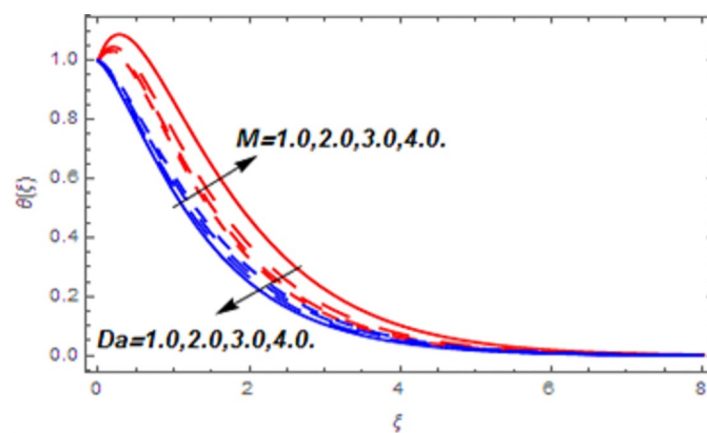
**Fig 7. Thermal profiles versus Darcy number and magnetic parameter.**
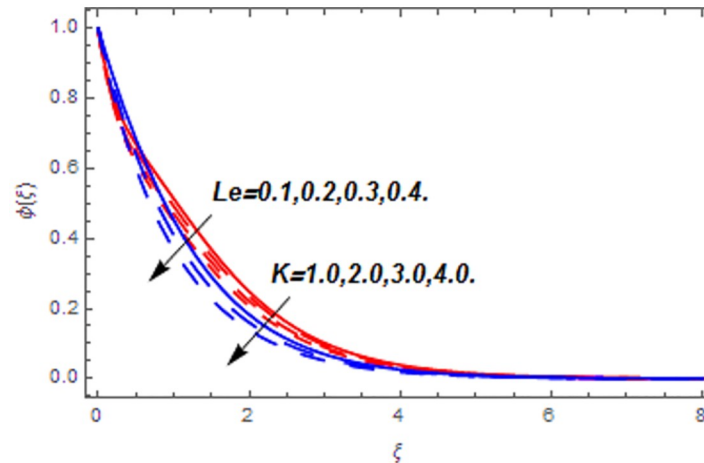
Fig 8. Concentration profiles versus Lewis number and chemical reaction parameter.

extension in magnetic parameter leads to generation of Lorentz force that causes a reduction in the flow profile due to resistive force. In this process a maximum heat flow takes place and causes an augmentation in thermal profile. Fig 8 expresses the upshot of Lewis number Le and chemical reaction factor K upon concentration profiles. The augmenting values of Le and K causes a reduction in the diffusivity of mass of fluid, due to which less transmission of mass takes place that weakens the concentration boundary layer thickness. On the other hand, the molecular diffusivity also suppresses with the growing in chemical reaction term which eventually decays the concentration of the fluid flow. Therefore, a declining impact is depicted here. Fig 9 examines the impacts of Brownian motion Nb and thermophoresis factor Nt upon the concentration profiles. The higher values of Nb has a reverse impact on the mass transfer. Actually, with the augmentation in Nb the random motion boosts due to which fluid particles are colliding more frequently. In this phenomenon more resistance is experienced by the fluid motion that weakens the concentration boundary layer thickness that ultimately drops the mass profile as portrayed in Fig 9. The concentration gradient within the fluid particles
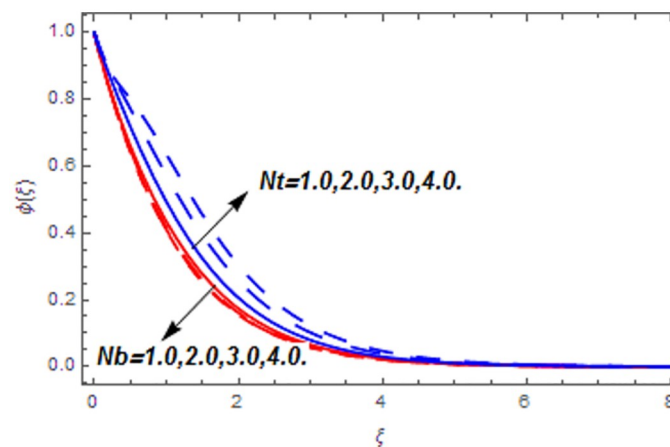
Fig 9. Concentration profiles versus Brownian motion and thermophoresis parameters.
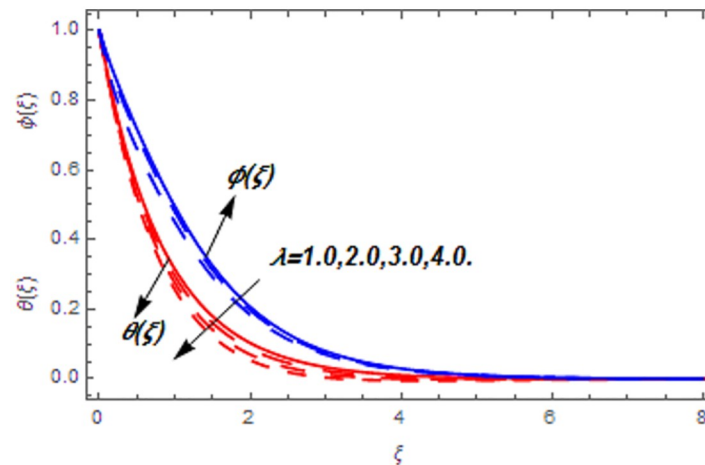
Fig 10. Impact of stretching parameter on thermal and concentration profiles.

maximizes for higher values of Nt, due to which more mass transfers from higher to lower concentration region. In this physical process concentration profiles grow up. Fig 10 demonstrates the influence of stretching parameter λ upon the energy and mass profiles. Form this figure it is observed that the higher values of λ has an adverse effect upon both profiles. Actually, the increasing stretching parameter decrease the thermal and mass boundary layer thicknesses and thus the thermal and concentration profiles decline. Fig 11a–11d displays the impact of magnetic field on streamlines. Fig 11a shows the streamlines of the Casson fluid for the case of non-magnetized flow. Here, the streamlines are close to each other which show the heightening impact in velocity of the Casson fluid flow. Fig 11b–11d shows the streamlines of the Casson fluid for the case of magnetized flow. Here, for the increasing magnetic field, the streamlines becomes apart from each other which shows the reducing impact in velocity of the Casson fluid flow. Actually, the greater magnetic field produces resistive force to the fluid flow which reduces the velocity profile of the fluid flow. The surface drag force, heat, and mass transfer rates are calculated through a numerical approach and are displayed in Table 2. The resistive forces augmented with the rising values of β, M, and Da, while the drag force fall due to the higher values of Rd and Ec. In fact, the viscous forces are not dominant in the presence of the accumulative values of these parameters. Similarly, the heat transmission rate reduce due the larger amount of β and Da, while show dominancy in the case of the larger values of Rd, Ec, M, Nt and Nb. The mass transport rate decline with the increasing values of Le and Nt, while rises with the greater values of Nb.

6. Conclusion

This work describes the improvement of energy and mass transmission for a mixed convection Casson fluid flow upon a stretching porous sheet. The fluid flow is considered with the impacts of thermophoresis and Brownian motion by using the idea of Buongiorno's model. The influence of chemical reactions has also been incorporated in the concentration equation. The equations that regulate the flow problem have been transmuted to dimensionless forms by using suitable similarity variables. The solution has been determined by HAM. The impact of numerous substantial constraints upon different profiles of the flow systems has been discussed in detail. The key points of the proposed analysis are listed as:

(a) $M = 0$

(b) $M = 1$

(c) $M = 5$

(d) $M = 10$
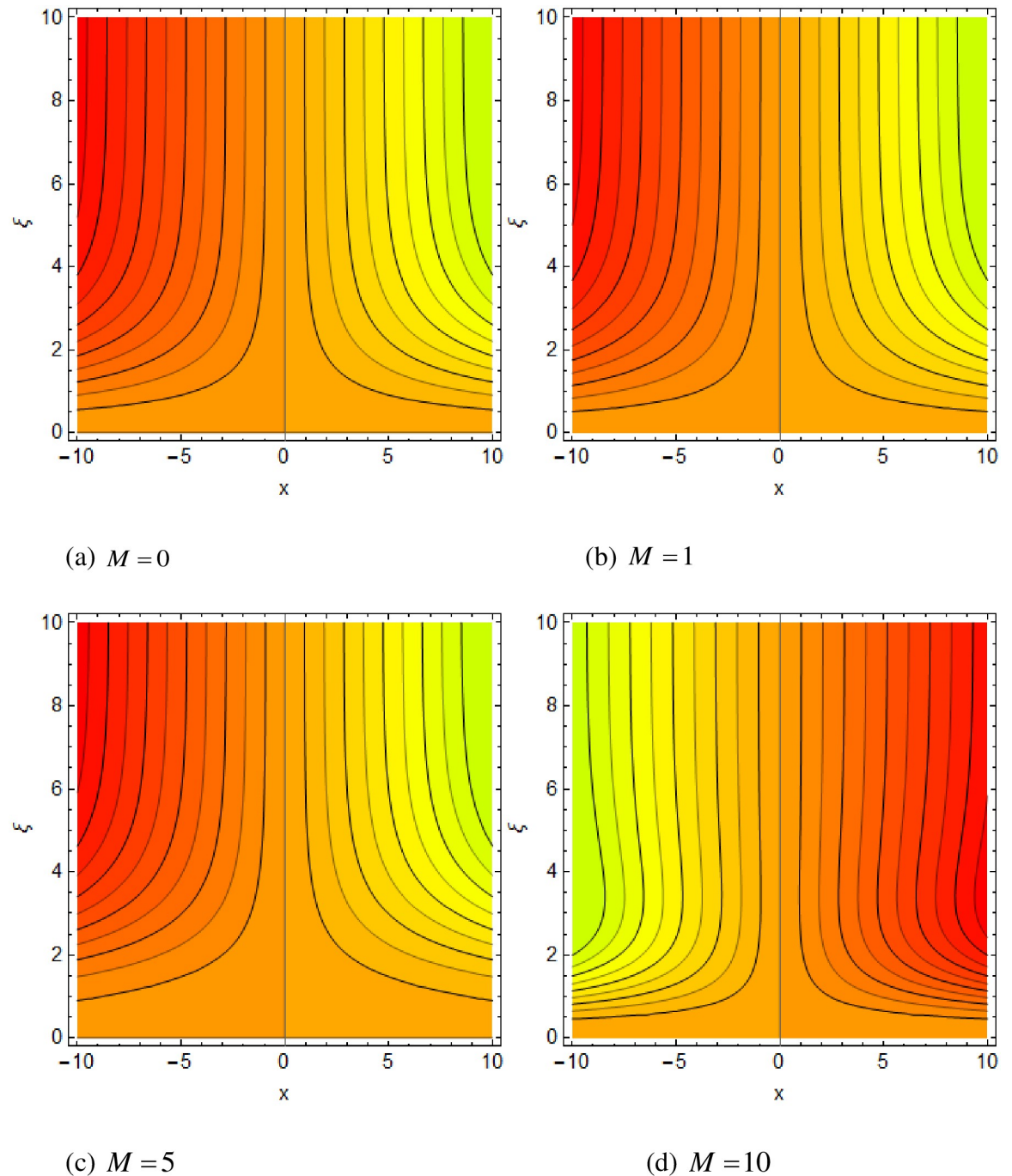
Fig 11. (a–d) Impact of magnetic field on streamlines when Pr = 5.0, λ = 0.5, Da = 1.0, Ec = 0.1, Nb = 0.2, Nt = 0.2, Le = 0.3, Nr = 0.2, Rd = 1.3 and Ra = 10^3.

https://doi.org/10.1371/journal.pone.0265238.g011

- The augmented Darcy number, Casson and magnetic parameters have declined the velocity of the Casson fluid flow.

- Growth in Brownian motion augments the chaotic motion amongst the particles, due to which the kinetic energy of particles transforms to heat energy which consequently augmented the thermal profile, while reduced the concentration profile.

Table 2. Statistical assessments of skin friction, energy transition and mass transmission rates.

β	Da	M	Rd	Ec	Nb	Nt	Le	$\left(1+\frac{1}{\beta}\right)f''(0)$	$-\left(1+\frac{4}{3}Rd\right)\theta'(0)$	$-\phi'(0)$
0.1	0.1	0.1	0.1	0.1	0.1	0.1	0.1	0.83827	1.73421	1.68537
0.2								0.97432	1.70053	1.68537
0.3								1.09264	1.62473	1.68537
	0.2							0.97630	1.72243	1.68537
	0.3							1.187614	1.71731	1.68537
		0.2						1.034123	1.74213	1.68537
		0.3						1.376413	1.75102	1.68537
			0.2					0.83716	1.842301	1.68537
			0.3					0.83802	1.95042	1.68537
				0.2				0.837231	1.78337	1.68537
				0.3				0.836012	1.83341	1.68537
					0.2			0.83827	1.75431	1.77143
					0.3			0.83827	1.77523	1.89331
						0.2		0.83827	1.78783	1.65431
						0.3		0.83827	1.83910	1.62402
							0.2	0.83827	1.73421	1.55268
							0.3	0.83827	1.73421	1.42423

https://doi.org/10.1371/journal.pone.0265238.t002

- Augmentation in thermophoresis parameter has increased the temperature and concentration profiles.

- The augmented radiation parameter, magnetic parameter, and Eckert number have augmented the thermal profile, while the higher Darcy number has declined the thermal profile.

- The growing values of Lewis number and chemical reaction parameter cause a reduction in the diffusivity of mass of fluid, due to which less transfer of mass takes place that weakens the concentration layer thickness and declines the concentration profiles.

- The higher stretching parameter has declined the thermal and concentration profiles.

Author Contributions

Conceptualization: Anwar Saeed.

Formal analysis: Musaad S. Aldhabani.

Funding acquisition: Poom Kumam.

Investigation: Abdullah Dawar.

Methodology: Abdullah Dawar.

Project administration: Poom Kumam.

Resources: Wiyada Kumam.

Software: Abdullah Dawar.

Validation: Ebrahem A. Algehyne, Musaad S. Aldhabani, Wiyada Kumam.

Visualization: Ebrahem A. Algehyne.

Writing – original draft: Anwar Saeed.

Writing – review & editing: Ebrahem A. Algehyne, Musaad S. Aldhabani.

References

1. Carbonell R. G., & Whitaker S. (1984). Heat and mass transfer in porous media. In Fundamentals of transport phenomena in porous media (pp. 121–198). Springer, Dordrecht.

2. Yaglom A. M., & Kader B. A. (1974). Heat and mass transfer between a rough wall and turbulent fluid flow at high Reynolds and Peclet numbers. Journal of Fluid Mechanics, 62(3), 601–623.

3. Bandaru M., Rashidi M. M., & Raju H. S. (2017). Influence of nonliner convection and thermophoresis on heat and mass transfer from a rotating cone to fluid flow in porous medium. Thermal Science, 21(6 Part B), 2781–2793.

4. Krishna M. V., Jyothi K., & Chamkha A. J. (2020). Heat and mass transfer on MHD flow of second-grade fluid through porous medium over a semi-infinite vertical stretching sheet. Journal of Porous media, 23(8).

5. Ahmad S., Ali K., Rizwan M., & Ashraf M. (2021). Heat and mass transfer attributes of copper–aluminum oxide hybrid nanoparticles flow through a porous medium. Case Studies in Thermal Engineering, 25, 100932.

6. Buongiorno J. (2006). Convective transport in nanofluids.

7. Tiwari R. K., & Das M. K. (2007). Heat transfer augmentation in a two-sided lid-driven differentially heated square cavity utilizing nanofluids. International Journal of heat and Mass transfer, 50(9–10), 2002–2018.

8. Khan A., Saeed A., Gul T., Mukhtar S., Ali I., & Jawad M. (2021). Radiative swirl motion of hydromagnetic Casson nanofluid flow over rotary cylinder using Joule dissipation impact. Physica Scripta, 96(4), 045206.

9. Khan A., Saeed A., Tassaddiq A., Gul T., Kumam P., Ali I., et al. (2021). Bio-convective and chemically reactive hybrid nanofluid flow upon a thin stirring needle with viscous dissipation. Scientific reports, 11 (1), 1–17.

10. Khan A., Saeed A., Tassaddiq A., Gul T., Mukhtar S., Kumam P., et al. (2021). Bio-convective micropolar nanofluid flow over thin moving needle subject to Arrhenius activation energy, viscous dissipation and binary chemical reaction. Case Studies in Thermal Engineering, 25, 100989.

11. Khan A., Kumam W., Khan I., Saeed A., Gul T., Kumam P., et al. (2021). Chemically reactive nanofluid flow past a thin moving needle with viscous dissipation, magnetic effects and hall current. Plos one, 16 (4), e0249264. https://doi.org/10.1371/journal.pone.0249264 PMID: 33857175

12. Mittal A. S., & Patel H. R. (2020). Influence of thermophoresis and Brownian motion on mixed convection two dimensional MHD Casson fluid flow with non-linear radiation and heat generation. Physica A: Statistical Mechanics and its Applications, 537, 122710.

13. Ashraf K., Siddique I., & Hussain A. (2020). Impact of thermophoresis and brownian motion on non-Newtonian nanofluid flow with viscous dissipation near stagnation point. Physica Scripta, 95(5), 055217.

14. Abdelmalek Z., Hussain A., Bilal S., Sherif E. S. M., & Thounthong P. (2020). Brownian motion and thermophoretic diffusion influence on thermophysical aspects of electrically conducting viscoinelastic nanofluid flow over a stretched surface. Journal of Materials Research and Technology, 9(5), 11948–11957.

15. Rashidi MM, Nazari MA, Mahariq I, Assad MEH, Ali ME, Almuzaiqer R, et al. Thermophysical Properties of Hybrid Nanofluids and the Proposed Models: An Updated Comprehensive Study. *Nanomaterials*. 2021; 11(11):3084. https://doi.org/10.3390/nano11113084 PMID: 34835847

16. Ramezanizadeh Mahdi, Nazari Mohammad Alhuyi, Modeling thermal conductivity of Ag/water nanofluid by applying a mathematical correlation and artificial neural network, *International Journal of Low-Carbon Technologies*, Volume 14, Issue 4, December 2019, Pages 468–474, https://doi.org/10.1093/ijlct/ctz030

17. Gangadhar K., & Bhaskar R. N. (2013). Chemically reacting MHD boundary layer flow of heat and mass transfer over a moving vertical plate in a porous medium with suction.

18. Seth G. S., Hussain S. M., & Sarkar S. (2015). Hydromagnetic natural convection flow with heat and mass transfer of a chemically reacting and heat absorbing fluid past an accelerated moving vertical plate with ramped temperature and ramped surface concentration through a porous medium. Journal of the Egyptian Mathematical Society, 23(1), 197–207.

19. Reddy P. S., Sreedevi P., & Chamkha A. J. (2017). MHD boundary layer flow, heat and mass transfer analysis over a rotating disk through porous medium saturated by Cu-water and Ag-water nanofluid with chemical reaction. Powder technology, 307, 46–55.

20. Raju R. S. (2018). Unsteady MHD boundary layer flow of Casson fluid over an inclined surface embedded in a porous medium with thermal radiation and chemical reaction. Journal of Nanofluids, 7(4), 694–703.

21. Punith Gowda R. J., Naveen Kumar R., Jyothi A. M., Prasannakumara B. C., & Sarris I. E. (2021). Impact of binary chemical reaction and activation energy on heat and mass transfer of marangoni driven boundary layer flow of a non-Newtonian nanofluid. Processes, 9(4), 702.

22. Mabood F., Shateyi S., Rashidi M. M., Momoniat E., & Freidoonimehr N. J. A. P. T. (2016). MHD stagnation point flow heat and mass transfer of nanofluids in porous medium with radiation, viscous dissipation and chemical reaction. Advanced Powder Technology, 27(2), 742–749.

23. Shah Z., Kumam P., & Deebani W. (2020). Radiative MHD Casson Nanofluid Flow with Activation energy and chemical reaction over past nonlinearly stretching surface through Entropy generation. Scientific reports, 10(1), 1–14.

24. Noor N. A. M., Shafie S., & Admon M. A. (2020). Unsteady MHD squeezing flow of Jeffrey fluid in a porous medium with thermal radiation, heat generation/absorption and chemical reaction. Physica Scripta, 95(10), 105213.

25. Dagana J., & Amos E. (2020). MHD Free Convection Heat and Mass Transfer flow in a Porous Medium with Dufour and Chemical reaction Effects.

26. Hussain S. M., Jain J., Seth G. S., & Rashidi M. M. (2017). Free convective heat transfer with Hall effects, heat absorption and chemical reaction over an accelerated moving plate in a rotating system. Journal of Magnetism and Magnetic Materials, 422, 112–123.

27. Bejan A., & Khair K. R. (1985). Heat and mass transfer by natural convection in a porous medium. International Journal of Heat and Mass Transfer, 28(5), 909–918.

28. Chaudhary R. C., & Jain A. (2007). Combined heat and mass transfer effects on MHD free convection flow past an oscillating plate embedded in porous medium. Romanian Journal of Physics, 52(5–7), 505–524.

29. Jiang X., Zhang H., & Wang S. (2020). Unsteady magnetohydrodynamic flow of generalized second grade fluid through porous medium with Hall effects on heat and mass transfer. Physics of Fluids, 32 (11), 113105.

30. Kumar M. A., Reddy Y. D., Goud B. S., & Rao V. S. (2021). Effects of soret, dufour, hall current and rotation on MHD natural convective heat and mass transfer flow past an accelerated vertical plate through a porous medium. International Journal of Thermofluids, 9, 100061.

31. Haq R. U., Raza A., Algehyne E. A., & Tlili I. (2020). Dual nature study of convective heat transfer of nanofluid flow over a shrinking surface in a porous medium. International Communications in Heat and Mass Transfer, 114, 104583.

32. Das S., Sahoo R.K., Effect of Darcy, fluid rayleigh and heat generation parameters on natural convection in a porous square enclosure: A Brinkman-extended Darcy model, International Communications in Heat and Mass Transfer, Volume 26, Issue 4, 1999, Pages 569–578, https://doi.org/10.1016/S0735-1933(99)00043-3

33. Sankad G. C., Maharudrapppa I., and Dhange M. Y., Bioconvection In Casson Fluid Flow With Gyrotactic Microorganisms And Heat Transfer Over A Linear Stretching Sheet In Presence Of Magnetic Field. Advances in Mathematics: Scientific Journal 10 (2021), no.1, 155–169 https://doi.org/10.37418/amsj.10.1.16

34. Makinde O.D., Khan W.A., Khan Z.H. Buoyancy effects on MHD stagnation point flow and heat transfer of a nanofluid past a convectively heated stretching/shrinking sheet, International Journal of Heat and Mass Transfer, 62, 2013, 526–533, https://doi.org/10.1016/j.ijheatmasstransfer.2013.03.049